and bulbar muscular atrophy. J Neurol Sci 1996;135:43–50.
19. Makiyama T, Akao M, Tsuji K, et al. High risk for bradyarrhythmic complications in patients with Brugada syndrome caused by SCN5A gene mutations. J Am Coll Cardiol 2005;46:2100–2106.
20. Fukuyama M, Ohno S, Wang Q, et al. L-type calcium channel mutations in Japanese patients with inherited arrhythmias. Circ J 2013;77:1799–1806.
21. Atsuta N, Watanabe H, Ito M, et al. Natural history of spinal and bulbar muscular atrophy (SBMA): a study of 223 Japanese patients. Brain 2006;129:1446–1455.
22. Fernandez-Rhodes LE, Kokkinis AD, White MJ, et al. Efficacy and safety of dutasteride in patients with spinal and bulbar muscular atrophy: a randomised placebo-controlled trial. Lancet Neurol 2011;10:140–147.
23. Morimoto S, Uemura A, Hishida H. An autopsy case of Brugada syndrome with significant lesions in the sinus node. J Cardiovasc Electrophysiol 2005;16:345–347.
24. Asai H, Hirano M, Udaka F, et al. Sympathetic disturbances increase risk of sudden cardiac arrest in sporadic ALS. J Neurol Sci 2007;254:78–83.
25. Mizusawa Y, Wilde AA. Brugada syndrome. Circ Arrhythm Electrophysiol 2012;5:606–616.
26. Veerakul G, Nademanee K. Brugada syndrome: two decades of progress. Circ J 2012;76:2713–2722.
27. Matsuo K, Akahoshi M, Nakashima E, et al. The prevalence, incidence and prognostic value of the Brugada-type electrocardiogram: a population-based study of four decades. J Am Coll Cardiol 2001;38:765–770.
28. Sakabe M, Fujiki A, Tani M, Nishida K, Mizumaki K, Inoue H. Proportion and prognosis of healthy people with coved or saddle-back type ST segment elevation in the right precordial leads during 10 years follow-up. Eur Heart J 2003;24:1488–1493.
29. Schmidt BJ, Greenberg CR, Allingham-Hawkins DJ, Spriggs EL. Expression of X-linked bulbospinal muscular atrophy (Kennedy disease) in two homozygous women. Neurology 2002;59:770–772.
30. Katsuno M, Adachi H, Doyu M, et al. Leuprorelin rescues polyglutamine-dependent phenotypes in a transgenic mouse model of spinal and bulbar muscular atrophy. Nat Med 2003;9:768–773.
31. Chevalier-Larsen ES, O'Brien CJ, Wang H, et al. Castration restores function and neurofilament alterations of aged symptomatic males in a transgenic mouse model of spinal and bulbar muscular atrophy. J Neurosci 2004;24:4778–4786.
32. Nedelsky NB, Pennuto M, Smith RB, et al. Native functions of the androgen receptor are essential to pathogenesis in a Drosophila model of spinobulbar muscular atrophy. Neuron 2010;67:936–952.
33. Shimizu W, Matsuo K, Kokubo Y, et al. Sex hormone and gender difference: role of testosterone on male predominance in Brugada syndrome. J Cardiovasc Electrophysiol 2007;18:415–421.
34. Querin G, Melacini P, D'Ascenzo C, et al. No evidence of cardiomyopathy in spinal and bulbar muscular atrophy. Acta Neurol Scand 2013;128:e30–e32.
35. Gallagher MM, Forleo GB, Behr ER, et al. Prevalence and significance of Brugada-type ECG in 12,012 apparently healthy European subjects. Int J Cardiol 2008;130:44–48.
36. Bezzina CR, Barc J, Mizusawa Y, et al. Common variants at SCN5A-SCN10A and HEY2 are associated with Brugada syndrome, a rare disease with high risk of sudden cardiac death. Nat Genet 2013;45:1044–1049.
37. Calloe K, Refaat MM, Grubb S, et al. Characterization and mechanisms of action of novel NaV1.5 channel mutations associated with Brugada syndrome. Circ Arrhythm Electrophysiol 2013;6:177–184.
38. Mo K, Razak Z, Rao P, et al. Microarray analysis of gene expression by skeletal muscle of three mouse models of Kennedy disease/spinal bulbar muscular atrophy. PLoS One 2010;5:e12922.
39. Minamiyama M, Katsuno M, Adachi H, et al. Naratriptan mitigates CGRP1-associated motor neuron degeneration caused by an expanded polyglutamine repeat tract. Nat Med 2012;18:1531–1538.
40. Mok NS, Tong CK, Yuen HC. Concomitant-acquired long QT and Brugada syndromes associated with indapamide-induced hypokalemia and hyponatremia. Pacing Clin Electrophysiol 2008;31:772–775.

The Premier Event for *the* Latest Research on Concussion

Registration is now open for The Sports Concussion Conference—*the* premier event on sports concussion from the American Academy of Neurology—set for July 11 through 13, 2014, at the Sheraton Chicago Hotel & Towers in Chicago. You won't want to miss this one-of-a-kind opportunity to learn the very latest scientific advances in diagnosing and treating sports concussion, post-concussion syndrome, chronic neurocognitive impairment, and controversies around gender issues and second impact syndrome from the world's leading experts on sports concussion. Early registration ends June 9, 2014. Register today at *AAN.com/view/ConcussionConference.*

misfolded proteins and may play a role in protecting neuronal cells against the toxic properties of polyQ expansions (9–11). The carboxyl terminus of the Hsc70-interacting protein (CHIP), a U-box-type E3 ubiquitin ligase, interacts with heat shock protein 90 (Hsp90) or Hsp70 and ubiquitylates and degrades unfolded proteins that are trapped by molecular chaperones. Thus, CHIP acts as a 'quality-control E3' (12). Macroautophagy is a set of bulk degradation processes in which cells form double-membrane vesicles, called autophagosomes, around a portion of the cytoplasm. These autophagosomes ultimately fuse with lysosomes, resulting in the degradation of their substrates. The microtubule-associated protein light-chain 3 (LC3)-II specifically associates with autophagosomes, and thus, the levels of LC3-II are correlated with the number of autophagic vacuoles (13). The transcription factor EB (TFEB) regulates autophagy by upregulating genes that belong to the coordinated lysosomal expression and regulation (CLEAR) network (14,15), which thereby controls lysosomal biogenesis.

Paeoniflorin (PF) is the principal active ingredient extracted from the roots of *Paeonia* plants, including *Paeonia alba* and *Paeonia lactiflora*. PF has been shown to have various biological and biomodulating activities, including the improvement of memory, antioxidant activity, antiepileptic activity, anti-stroke properties and anti-neuroinflammation. Several studies have suggested that PF upregulates the expression of molecular chaperones and LC3-II and enhances the degradation of disease-causative proteins via the proteolytic machinery, indicating that PF may have neuroprotective effects (16,17). However, the possible implications for neuronal disease treatment have not been assessed in models of disease, and the mechanisms underlying the activation of the proteolytic machinery are not understood.

Here, we present findings supporting the concept of a proteolytic, machinery-dependent pathophysiology in a neurodegenerative disease. We examined the effects of PF in cultured cells and the transgenic mouse model of SBMA. PF administration inhibited the nuclear accumulation of the mutant AR and significantly ameliorated the motor phenotype of the SBMA mouse model without detectable toxicity. Mutant AR was preferentially degraded over wild-type AR in the presence of PF in both cell culture and mouse models of SBMA. PF significantly induced nuclear factor-YA (NF-YA), also known as CCAAT box-binding factor (CBF) (18,19), resulting in the upregulation of the molecular chaperones CHIP and TFEB. Furthermore, because this proteolytic machinery is considered to be an effect common to other polyQ diseases, our observations suggest that PF is a promising therapeutic candidate for a wide range of polyQ-mediated neurodegenerative diseases, including SBMA. PF enhanced two major proteolysis systems, the molecular chaperone–UPS and the autophagy system. Thus, we demonstrated that PF promoted the degradation of mutant AR to a greater extent than the induction of either the molecular chaperone–UPS or the autophagy system alone.

RESULTS

PF preferentially reduces the amount of polyQ-expanded mutant AR by integrating into the proteolytic machinery

To examine the efficacy of PF in promoting the degradation of mutant polyQ-expanded AR, we treated NSC34 cells stably expressing the wild-type (AR-24Q) or mutant AR (AR-97Q) with the indicated doses of PF or phosphate buffered saline (PBS) for 24 h. Although the anti-AR immunoblot showed a dose-dependent decline in both wild-type and mutant AR expression in response to PF (Fig. 1A), the decrease in monomeric mutant AR (62.8% at 10 μM PF) was significantly greater than that of wild-type AR (31.3%; Fig. 1B). These data suggest that the accumulation of mutant AR is selectively reduced at higher levels in response to PF than wild-type AR ($P < 0.01$). A similar preferential reduction in mutant AR was observed in another cell model expressing transiently transfected ARs (Supplementary Material, Fig. S1A and B). To reveal the mechanism underlying the PF-induced activation of the proteolytic machinery and the enhancement of the degradation of the mutant AR, we screened the expression of key transcription factors and molecules, which trigger the induction of the molecular chaperone–UPS or autophagy (or both), in the cell culture and transgenic mouse models of SBMA expressing AR-24Q. Among these factors, PF treatment significantly increased the expression level of two transcription factors, NF-YA and TFEB (Supplementary Material, Fig. S2A–D). PF treatment also significantly increased the expression levels of molecular chaperones and CHIP in a dose-dependent manner (Fig. 1A and B), and it also upregulated NF-YA mRNA (Fig. 1C). However, there were no significant differences in the expression levels of these molecules between cells expressing the wild-type or mutant AR (Fig. 1B). There was also no deterioration of cell viability after PF treatment in cells that stably expressed either wild-type or mutant AR (Supplementary Material, Fig. S3). These data indicate that PF preferentially degrades the mutant AR protein without cellular toxicity. Luciferase activity assays revealed that PF increased the transactivation of NF-YA, TFEB, Hsp70 and CHIP in a dose-dependent manner (Fig. 1D). To determine whether the decrease in AR was due to protein degradation or changes in RNA expression, the turnover of wild-type and mutant AR was assessed with a pulse-chase labeling assay. Without treatment, the wild-type and mutant AR were degraded to levels similar to those reported previously (20). However, in the presence of PF, both proteins had shortened half-lives. The wild-type AR decreased from ~6.5 to 5.5 h, and the mutant AR decreased from 5.5 to 3.5 h (Fig. 1E and F). The mRNA expression levels of both the wild-type and mutant AR were similar (Fig. 1G). The degradation of mutant AR by PF was inhibited both by the proteasome inhibitor lactacystin and bafilomycin A1, a potent inhibitor of autophagy (Fig. 1F and H). This evidence suggests that the PF-induced degradation was dependent on both the proteasome and autophagy systems. These data indicate that PF is non-toxic and preferentially degrades the mutant AR protein without altering mRNA levels.

NF-YA regulates both the proteasomal and autophagic proteolytic machinery

We next addressed whether PF promotes the degradation of mutant, polyQ-expanded AR via the upregulation of transcription factor NF-YA. NSC34 cells stably expressing AR-97Q were transfected with the indicated amount of NF-YA or mock transfected and were analyzed 24 h later (Fig. 2A). Immunoblot analysis demonstrated a dose-dependent decline in mutant AR expression following NF-YA overexpression (Fig. 2A and B).

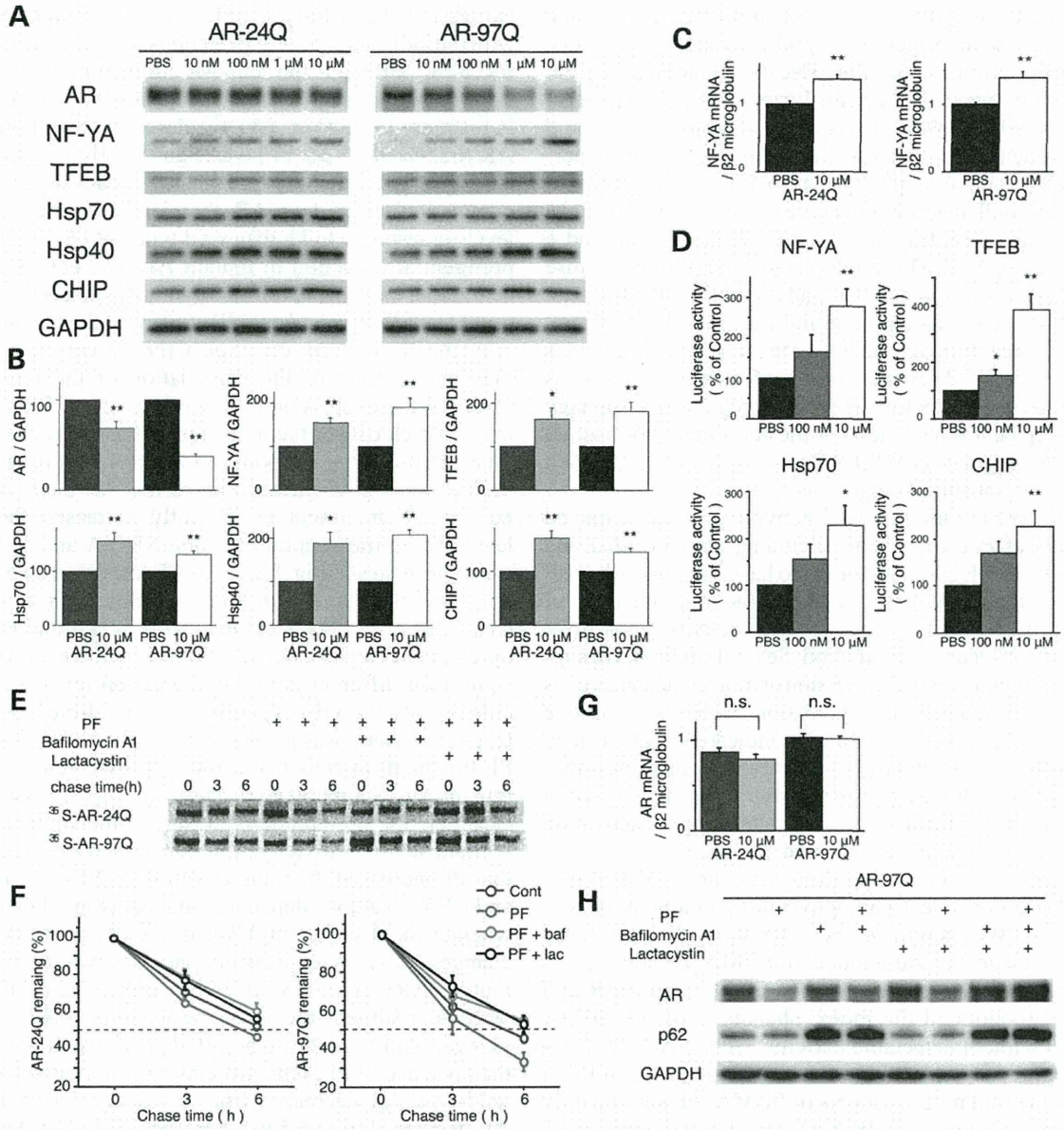

Figure 1. Effects of PF on AR in a cultured cell model of SBMA. (**A** and **B**) Western blots and densitometric analyses from NSC34 cells stably expressing wild-type (24Q) or mutant (97Q) AR (*$P < 0.05$; **$P < 0.01$, $n = 5$, unpaired *t*-test). (**C**) The expression level of NF-YA mRNA from NSC34 cells stably expressing wild-type (24Q) or mutant (97Q) AR (**$P < 0.01$, $n = 5$, unpaired *t*-test). (**D**) Constructs containing NF-YA, TFEB, Hsp70 or CHIP and a luciferase reporter gene were transfected into NSC34 cells. Luciferase activity assays were performed in triplicate in five independent experiments. Relative luciferase activity is represented as a ratio against the luciferase activity in cells transfected with an empty promoter vector (**$P < 0.01$, $n = 5$, one-way ANOVA with Tukey–Kramer *post hoc* test). (**E**) Pulse-chase analysis of two forms of AR. Data from one representative experiment for wild-type and mutant AR. Stably transfected NSC34 cells were treated with PF (10 μM), bafilomycin A1 (baf; 20 nM) and lactacystin (lac; 2.5 μM) for 16 h. (**F**) Pulse-chase assessment of the half-life of wild-type (left) and mutant AR (right). (**G**) Real-time RT–polymerase chain reaction (PCR) of wild-type and mutant AR mRNA. Quantities are presented as the ratio to β2 microglobulin mRNA. The wild-type and mutant AR mRNA levels were similar under PF treatments ($n = 5$, unpaired *t*-test). (**H**) Stably transfected NSC34 cells were treated with PF (10 μM), bafilomycin A1 (20 nM) and lactacystin (2.5 μM) for 16 h. Error bars (B, C, D, F, G), SEM.

The expression levels of Hsp70, CHIP and TFEB were also significantly increased following NF-YA overexpression (Fig. 2A and B). Moreover, the effects of PF were completely blocked in cells depleted of NF-YA (Fig. 2C and D), which suggests that PF primarily enhances mutant AR degradation through NF-YA upregulation and the downstream transactivation of the proteasomal and autophagic proteolytic machinery.

Effect of PF on expression levels of AR via TFEB activation *in vitro*

The aforementioned results demonstrate that PF increases the expression of TFEB, a master autophagy regulator, via the upregulation of NF-YA. TFEB translocates from the cytoplasm to the nucleus, which results in the activation of its target genes (14).

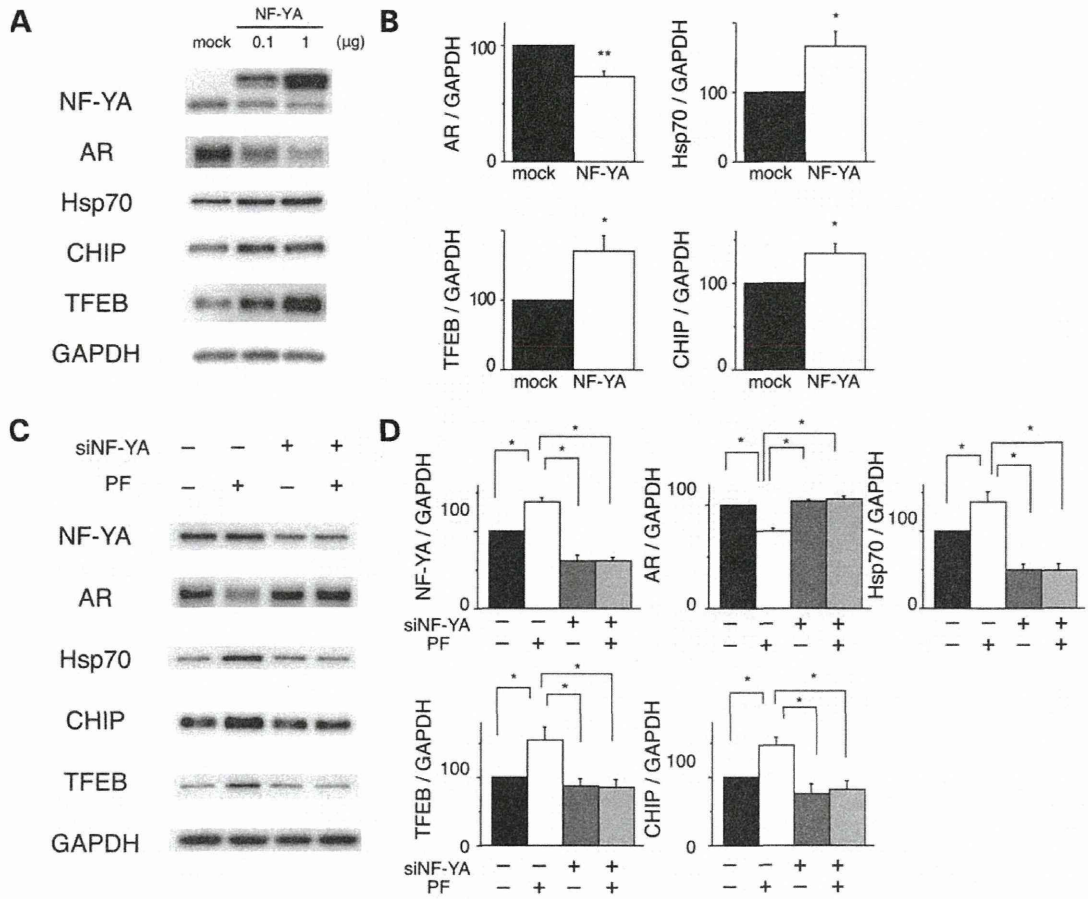

Figure 2. Effects of NF-YA overexpression in cultured cell models of SBMA. (**A** and **B**) Western blots and densitometric analyses of NSC34 cells stably expressing mutant AR. Cells were transfected with NF-YA with a V5 tag or the mock vector ($^{*}P < 0.05$; $^{**}P < 0.01$, $n = 5$, unpaired *t*-test). (**C** and **D**) Western blots and densitometric analyses of NSC34 cells stably expressing mutant AR that were transfected with control or NF-YA siRNA and treated with or without PF ($^{*}P < 0.05$, $n = 5$, one-way ANOVA with Tukey–Kramer *post hoc* test). Error bars (B and D), SEM.

We hypothesized that if PF contributes to the activation of autophagy, then the expression of the mutant polyQ protein would be reduced by TFEB-activated autophagy in addition to the UPS degradation. To test this hypothesis, the nuclear translocation of TFEB was investigated using western blot analysis, which showed that PF increased the amount of TFEB in the nucleus at a dose of 10 μM in NSC34 cells (Fig. 3A and B). Next, we investigated whether TFEB promotes the degradation of mutant AR. NSC34 cells stably expressing AR-24Q or AR-97Q were transfected with the indicated amount of TFEB or mock transfected (Fig. 3C). After 48 h, the expression levels of both AR-24Q and AR-97Q similarly decreased following the overexpression of TFEB (Fig. 3C and D). The expression of the autophagic marker LC3-II was significantly elevated in the cells expressing AR-24Q or AR-97Q (Fig. 3C and D), suggesting that the high expression of TFEB induced autophagosome formation and enhanced the degradation of the AR proteins. However, there were no significant differences in the reduction rate between the wild-type and mutant AR (Fig. 3C and D), which indicates that the activation of UPS is the basis for preferential degradation of the polyQ-expanded mutant AR following PF treatment.

PF ameliorates the phenotype of male AR-97Q mice

To verify that PF-mediated activation of the proteolytic machinery mitigates polyQ toxicity, we administered PF intraperitoneally every day at doses of 6.7 mg/kg (PF1) or 13.4 mg/kg (PF2) to males of the transgenic mouse model carrying the full-length human AR with either 24Q or 97Q (21). To demonstrate that PF slows the onset and progression of the disease, PF treatments were initiated when the mice reached 5 weeks of age and continued until they were 32 weeks old. The AR-97Q mice displayed progressive muscular atrophy and weakness that was accompanied by diffuse nuclear accumulation and NIs of mutant AR in neuronal and non-neuronal tissues (21). We examined various neurological and behavioral parameters. In the AR-97Q mice treated with 13.4 mg/kg PF (PF2), the phenotype and disease progression were markedly ameliorated, and the progression in mice treated with 6.75 mg/kg PF (PF1) was moderately ameliorated (Fig. 4A–F). The untreated AR-97Q mice (PF0) exhibited motor impairments (assessed by the rotarod task), as early as 9 weeks after birth, whereas the PF2 group showed initial impairments at 13 weeks after birth and had less deterioration than the PF0 mice (Fig. 4A). The PF1 mice exhibited intermediate levels of impairment in their

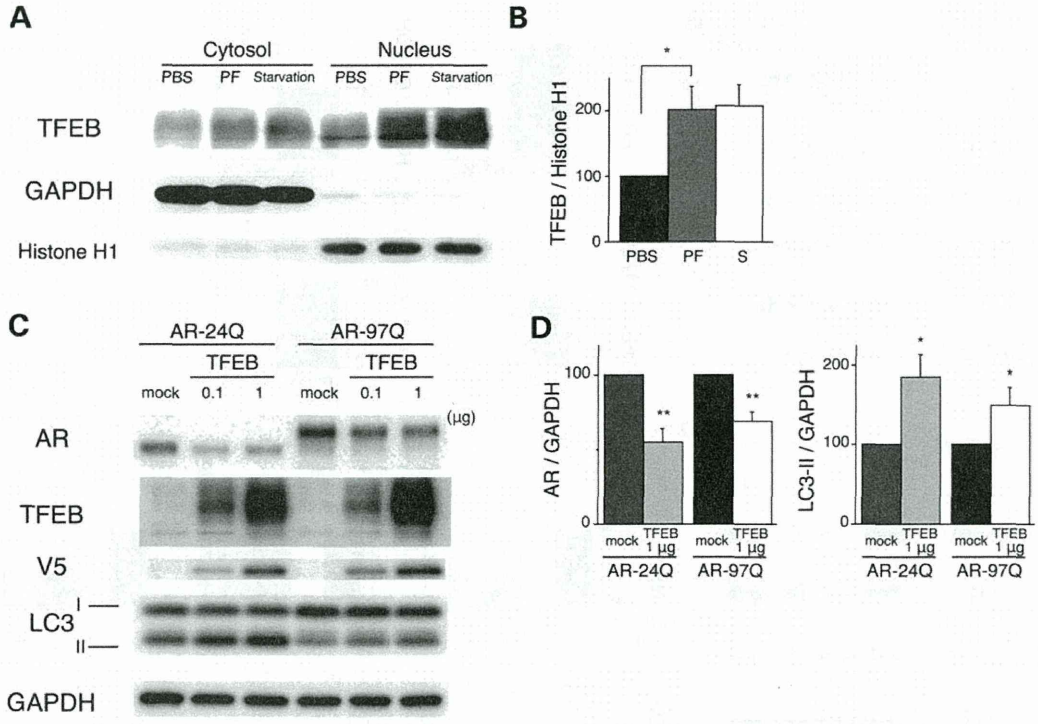

Figure 3. Effects of PF on expression levels of AR via TFEB activation. (**A** and **B**) PF facilitates the nuclear translocation of TFEB. Western blots and densitometric analyses from NSC34 cells treated with 10 μM PF or starvation. Cell lysates were subjected to nuclear or cytosolic fractionation and probed with a TFEB antibody. GAPDH and H1 were used as cytosolic and nuclear markers, respectively (*$P < 0.01, n = 5$, one-way ANOVA with Tukey–Kramer *post hoc* test). (**C** and **D**) Effects of TFEB overexpression on the expression levels of wild-type (24Q) and mutant (97Q) ARs in NCS34 cells. Western blots and densitometric analyses from NSC34 cells stably expressing AR-24Q or AR-97Q. Cells were transfected with the mock or TFEB-V5 vector (*$P < 0.01, n = 5$, unpaired *t*-test). Error bars (B and D), SEM.

rotarod performance (Fig. 4A). The locomotor cage activity of the PF0 mice was also markedly decreased at 15 weeks compared with the PF1 and PF2 groups, which exhibited decreases in activity at 24 and 26 weeks of age, respectively (Fig. 4B). No mouse lines were distinguishable in terms of body weight at birth; however, the PF0 mice lost weight significantly earlier (by 16 weeks) and to a greater extent than the PF1 and PF2 mice (Fig. 4C). PF treatment also significantly prolonged the lifespan of the PF1 and PF2 mice compared with the PF0 mice (Fig. 4D). Additionally, the PF0 mice exhibited motor weakness, as demonstrated by the dragging of their legs and shortened steps, whereas the PF2 mice had nearly normal ambulation (Fig. 4E and F). AR-24Q mice treated with PF did not have altered phenotypes (Supplementary Material, Fig. S4A–D). To evaluate the possible toxic effects of PF, we examined blood samples from 16-week-old AR-97Q mice treated with 13.4 mg/kg PF for 11 weeks. Measurements of aspartate aminotransferase, alanine aminotransferase, blood urea nitrogen and serum creatinine demonstrated that PF resulted in neither infertility nor liver or renal dysfunction in the AR-97Q male mice (Supplementary Material, Fig. S5A–D). The serum testosterone levels were unchanged in the PF2 mice (1.029 ± 0.369 ng/ml, $n = 15$) versus the PF0 mice (0.857 ± 0.406 ng/ml, $n = 15$).

PF reduces diffuse nuclear staining of mutant AR and degrades mutant AR protein in the mouse model of SBMA

Having demonstrated that PF promotes mutant AR degradation *in vitro*, we examined the levels of AR in the AR-24Q and AR-97Q mice. We performed immunohistochemical staining for mutant AR using the 1C2 antibody in the spinal cord and skeletal muscle of 16-week-old AR-97Q mice. In the PF0 mice, intense staining was frequently observed in the nuclei, whereas staining was infrequent in the PF1 mice and much less frequent in the PF2 mice (Fig. 5A). There were significantly more 1C2-positive cells in the spinal cord and muscle tissue of the PF0 mice than in the PF1 and PF2 mice (Fig. 5B). The 1C2-positive cell populations were not significantly different between the PF1 and PF2 mice (Fig. 5B). There were no NIs in the spinal cord and skeletal muscle of the AR-24Q mice (Supplementary Material, Fig. S4E and F).

Treatment with PF markedly diminished both the high-molecular-weight complex and monomeric mutant AR in the spinal cord and muscle of AR-97Q mice ($P < 0.01$). PF significantly diminished the wild-type monomeric AR in AR-24Q mice (Fig. 5C and D). In the PF2 mice, monomeric AR decreased by 68.5 and 34.5% in the spinal cord and by 50.3 and 37.2% in the skeletal muscle for the AR-97Q and AR-24Q mice, respectively (Fig. 5C and D). Thus, the rate of reduction of the monomeric mutant AR was significantly higher than for wild-type AR in both the spinal cord ($P < 0.01$) and skeletal muscle ($P < 0.01$). Reverse transcription (RT)–polymerase chain reaction (PCR) of both the AR-24Q and AR-97Q mice showed that the levels of AR mRNA were similar in the spinal cord and muscle of the treated (PF2) and untreated (PF0) mice (Fig. 5E and F); thus, the decreased

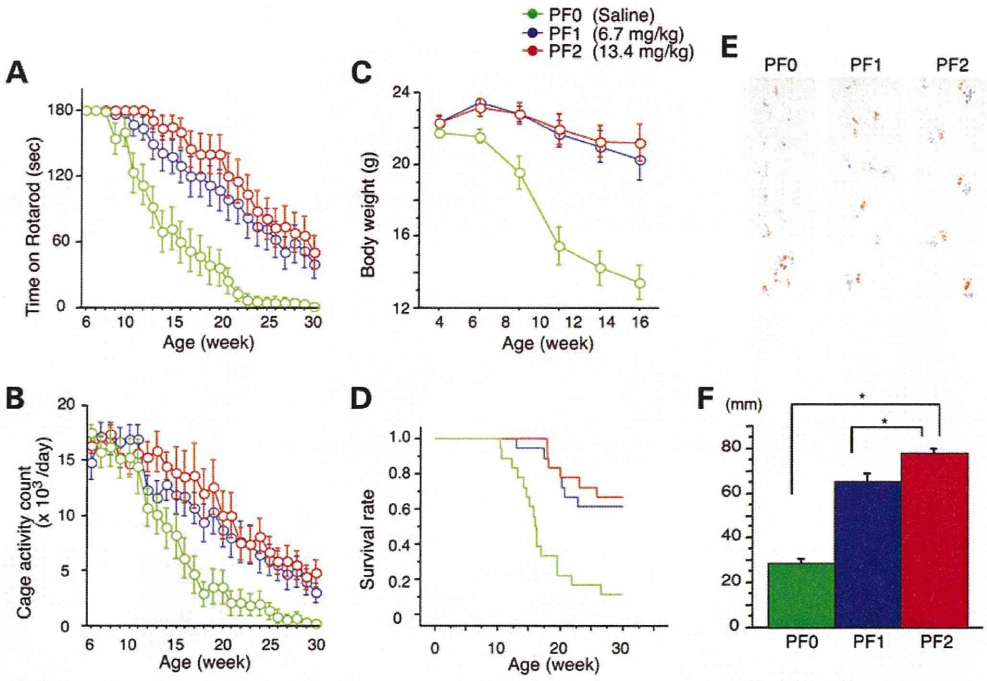

Figure 4. Effects of PF on behavioral phenotypes in AR-97Q mice. Untreated AR-97Q mice (PF0) or mice administered 6.7 mg/kg (PF1) or 13.4 mg/kg (PF2) PF intraperitoneally every day from ages 5 to 30 weeks were tested for rotarod performance (**A**), cage activity (**B**) and body weight (**C**). PF1 and PF2 mice remained on the rotarod longer and exhibited greater cage activity than PF0 mice. PF0 mice lost weight earlier than PF1 and PF2 mice. All parameters were significantly different in PF2 mice compared with PF0 mice: $P < 0.01$ at 25 weeks (rotarod and cage activity) and $P < 0.01$ at 10 weeks (body weight) ($n = 18$, two-way ANOVA with Tukey–Kramer *post hoc* test). (**D**) A Kaplan–Meier plot shows the prolonged survival of PF1 and PF2 mice compared with PF0 mice ($P = 0.0002$ and 0.0001, respectively; $n = 18$, log-rank test). (**E**) Footprints of representative 16-week-old AR-97Q mice treated with or without PF. Front paws are indicated in red, and hind paws are in blue. PF0 mice exhibited motor weakness, demonstrated by the dragging of the legs. PF1 mice walked with somewhat longer steps, and PF2 mice walked almost normally. (**F**) The length of the steps was measured in 16-week-old AR-97Q mice. Each column shows the average length of the steps of the hind paw. PF1 and PF2 mice walked with significantly longer steps than PF0 mice (*$P < 0.01$, $n = 6$, one-way ANOVA with Tukey–Kramer *post hoc* test). These data suggest that PF ameliorates the phenotypic expression of SBMA in AR-97Q mice in a dose-dependent manner. Error bars (F), SEM.

protein level was due to degradation and not to lower mRNA levels. These observations indicate that PF markedly degrades not only the high-molecular-weight mutant AR complex but also the monomeric mutant AR protein compared with the wild-type AR, which reflects the preferential degradation of the mutant AR through the UPS.

Anti-glial fibrillary acidic protein (GFAP) staining showed an apparent reduction in reactive astrogliosis in the PF2 mice in the spinal anterior horn (Fig. 5G). Muscle histology also demonstrated a marked amelioration of muscle atrophy in the PF2 mice (Fig. 5H).

Effect of PF on the regulation of proteolytic machinery *in vivo*

Both low and high doses of PF treatment of the SBMA transgenic mice were accompanied by marked increases in NF-YA mRNA levels and protein synthesis in the spinal cord and muscle tissue (Fig. 6A–F). These results were well correlated with those of anti-NF-YA immunohistochemical-stained tissue sections (Supplementary Material, Fig. S6A and B). In contrast, PF treatment in the cell and mouse models of SBMA had no effect on the expression levels of hyper-phosphorylated heat shock factor-1 (10,22), p53 (23) or transcription factors regulating Hsp expression, namely, TBP and SP1 (Supplementary Material, Fig. S2A). AR-97Q transgene expression decreased the expression level of NF-YA in both the spinal cord and muscle (Fig. 6C and D). This effect might be due to a decrease in mRNA levels (Fig. 6A and B) and sequestration of endogenous NF-YA in the inclusions in the spinal anterior horn cells and muscle tissue of AR-97Q mice; this finding was also observed in the spinal anterior horn cells of SBMA patients (Supplementary Material, Fig. S6A and B). To ensure that PF activated the proteolytic machinery *in vivo*, the expression levels of the molecular chaperones, CHIP and TFEB, were determined using western blotting. In the AR-24Q and AR-97Q mice, the levels of Hsp70, Hsp40, CHIP and TFEB were significantly increased (Fig. 6C–F), and PF facilitated the nuclear translocation of TFEB in the spinal cord and muscle of the AR-24Q and AR-97Q mice (Supplementary Material, Fig. S7). Furthermore, western blotting showed that PF treatment resulted in increased expression levels of lysosomal proteases and the autophagic marker LC3-II in the spinal cord and muscle of the AR-24Q and AR-97Q mice (Fig. 7A–D). The expression level of protease mRNA also increased in the AR-24Q and AR-97Q mice treated with 13.4 mg/kg PF as well as in the cell culture model treated with 10 μM PF (Supplementary Material, Fig. S8A–C). These observations suggest that an increase in the levels of the molecular chaperones CHIP and TFEB promotes the downregulation of ARs via the UPS and autophagic

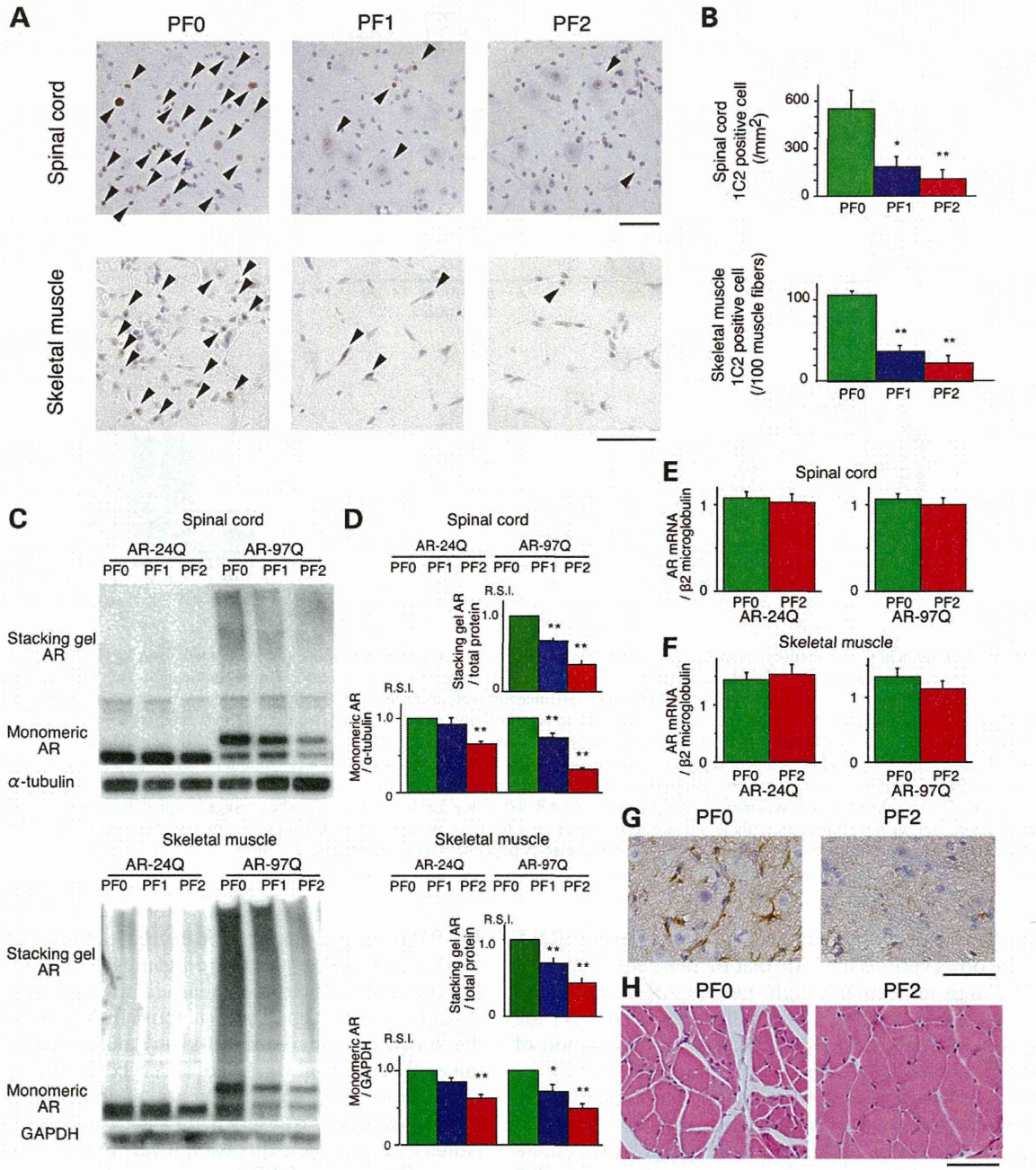

Figure 5. Effects of PF on the nuclear accumulation of abnormal AR in 16-week-old AR-24Q and AR-97Q mice. (**A**) Immunohistochemical staining for mutant AR using the 1C2 antibody showed a marked reduction in diffuse nuclear staining and NIs (arrow head) in the spinal cord and skeletal muscle of the treated mice compared with the PF0 mice. (**B**) Quantification of the number of 1C2-positive cells in the spinal cord and skeletal muscle of AR-97Q mice treated with or without PF ($^{*}P < 0.05$; $^{**}P < 0.01, n = 6$, one-way ANOVA with Tukey–Kramer *post hoc* test). (**C** and **D**) Western blot analysis of total tissue homogenates from the spinal cord and muscle of AR-24Q and AR-97Q mice probed with anti-AR ($^{*}P < 0.05$; $^{**}P < 0.01, n = 5$, one-way ANOVA with Tukey–Kramer *post hoc* test). (**E** and **F**) Real-time RT–PCR of wild-type and mutant AR mRNA in the spinal cord (E) and skeletal muscle (F). Quantities are presented as the ratio to β2 microglobulin mRNA ($n = 5$, unpaired *t*-test). (**G**) Immunohistochemical staining with anti-GFAP antibody in the spinal anterior horn of AR-97Q mice. (**H**) Hematoxylin and eosin staining of the muscles of AR-97Q mice. Error bars (B, D, E and F), SEM. Scale bars: 50 μm.

degradation. Collectively, these data suggest that the expression of molecules related to the proteolytic machinery is enhanced by PF treatment, which results in a heightened pharmacological effect. The expression of mutant AR is reduced, and the polyQ-dependent phenotype is mitigated by PF in the mouse model of SBMA.

DISCUSSION

Our results demonstrated that mutant AR is sensitive to PF treatment and that the PF-mediated downregulation of mutant AR can ameliorate motor abnormalities in an SBMA mouse model without detectable toxicity. PF treatment reduced the levels of

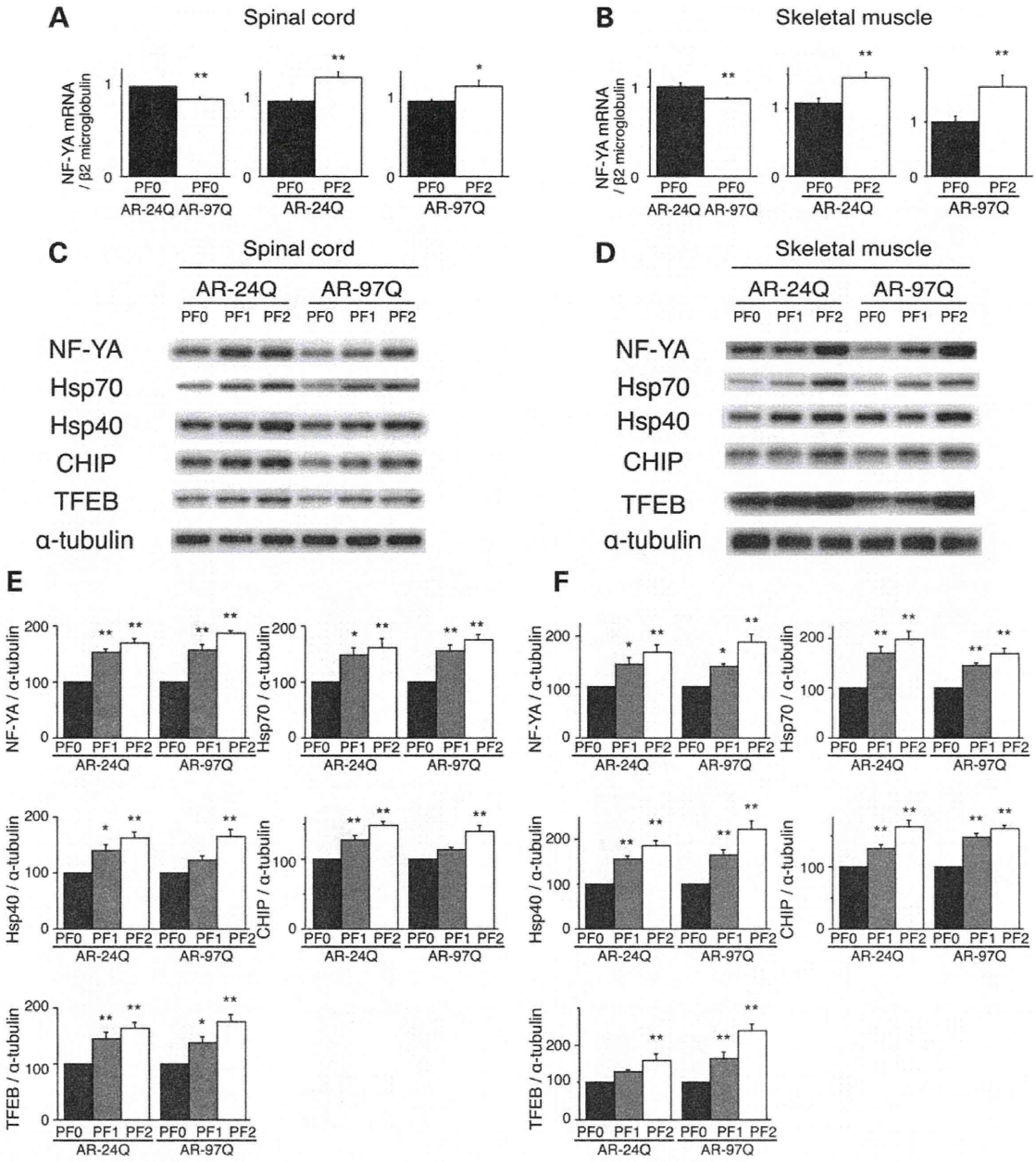

Figure 6. PF increased the expression of molecular chaperones, CHIP and transcription factors in AR-24Q mice and AR-97Q mice. The expression levels of NF-YA mRNA in the spinal cord (**A**) and skeletal muscle (**B**) of 16-week-old AR-24Q mice and AR-97Q mice ($^{**}P < 0.01$; $^{***}P < 0.001$, $n = 5$, unpaired *t*-test). Western blots and densitometric analyses of NF-YA, molecular chaperones, CHIP and TFEB in the spinal cord (**C** and **E**) and skeletal muscle (**D** and **F**) of 16-week-old AR-24Q mice and AR-97Q mice ($^{*}P < 0.05$; $^{**}P < 0.01$, $n = 5$, one-way ANOVA with Tukey–Kramer *post hoc* test). Error bars (A, B, E, F), SEM.

monomeric and aggregated forms of mutant AR. In chronic neurodegenerative disorders, such as polyQ diseases, Parkinson's disease, Alzheimer disease and amyotrophic lateral sclerosis, commonly observed phenotypes include the abnormal accumulation of disease-causing proteins and the formation of nuclear and cytoplasmic inclusions. Under pathologic conditions, the accumulated levels of misfolded and toxic proteins may exceed the protective ability of the proteolytic machinery; the inability to either maintain misfolded proteins in a soluble form or degrade them results in their accumulation and the formation of inclusions. In this study, we showed that PF potently induced a novel, NF-YA-mediated mechanism involving both the UPS and autophagy systems, which downregulated mutant AR accumulation and thereby ameliorated SBMA phenotypes in a mouse model. Motor neuron degeneration induced by mutant AR involves several distinct mechanisms, including transcriptional dysregulation, aggregate formation, impaired axonal transport, DNA binding and mitochondrial dysfunction. Although it remains unclear which of these mechanisms has a pivotal impact on SBMA pathogenesis, the accumulation of mutant AR is a well-established upstream molecular event of neuro- and myodegeneration (3). The successful anti-androgen

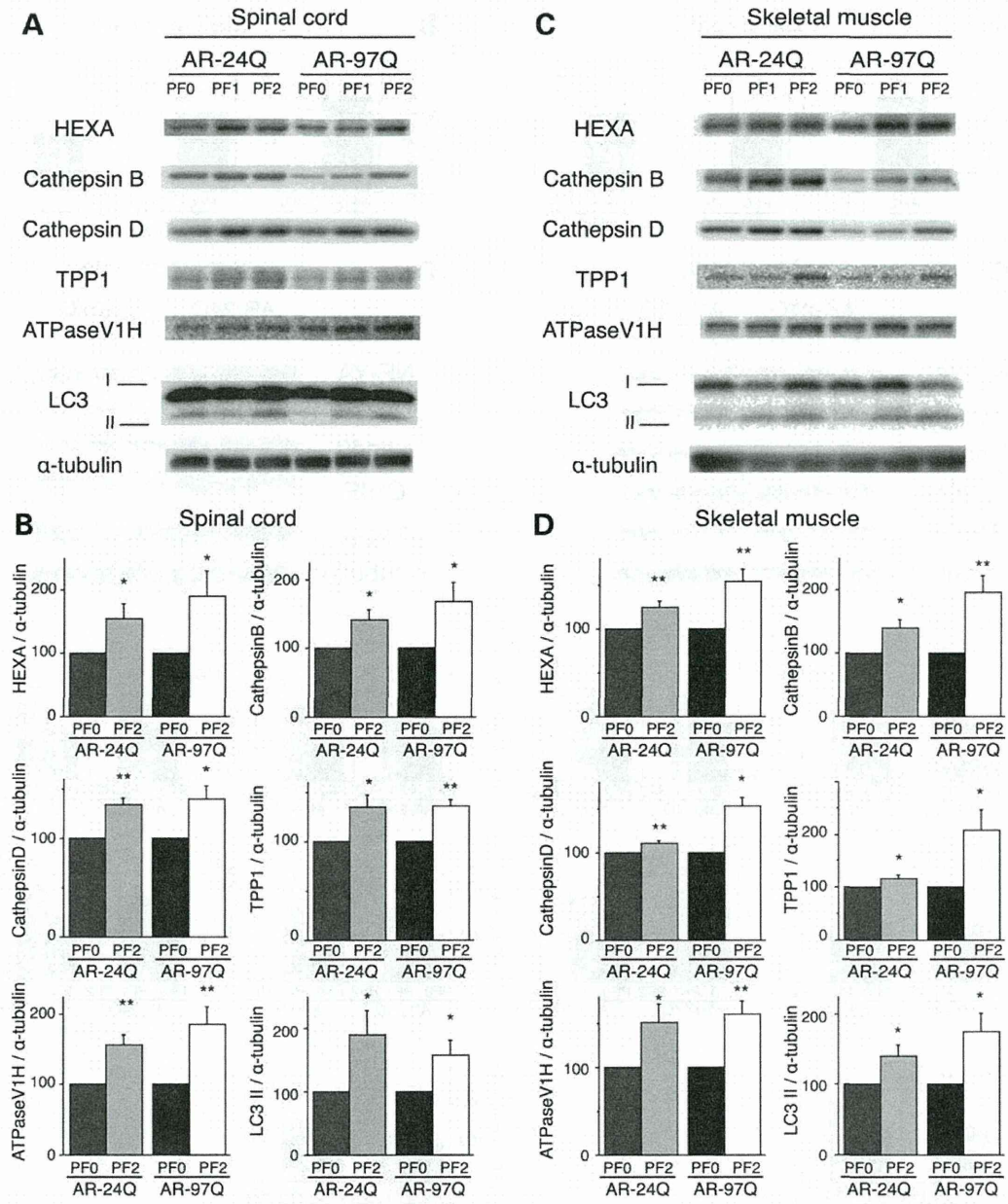

Figure 7. PF increased the expression of lysosomal proteases and LC3-*II* in AR-24Q and AR-97Q mice. Western blots and densitometric analyses for lysosomal proteases in the spinal cord (**A** and **B**) and skeletal muscle (**C** and **D**) of 16-week-old AR-24Q mice and AR-97Q mice ($^{*}P < 0.05$; $^{**}P < 0.01$, $n = 5$, unpaired *t*-test). Error bars (B, D), SEM.

therapy in SBMA mouse models has translated to clinical trials, which showed that swallowing function improved in patients with a disease duration of <10 years (24,25). Many studies have sought to elucidate the pathogenesis of polyQ diseases and develop treatment methods. Among these treatments, the pharmacologic induction of molecular chaperones, the UPS and autophagy may ameliorate these disorders (26). The mutant polyQ AR adopts an altered conformation that results in protein aggregation and inclusion formation; however, recent studies have suggested that soluble forms of the causative protein, including oligomeric protein, aggregate. Mutant monomers in the nuclear space may also be toxic (rather than protein inclusions). Thus, soluble protein aggregates, or possibly mutant monomers, represent targets in the treatment of neurodegenerative disorders (27–29). Indeed, we have demonstrated that reducing the levels of the pathogenic AR protein in SBMA mice attenuates the expression of the disease (30–35), which suggests that the clearance of mutant AR may therapeutically benefit SBMA. Our present data also confirm that PF passes through the blood–brain barrier and that long-term treatment with PF exerts significant pharmacological effects in the central nervous system.

NF-Y is a heterotrimeric complex that consists of three subunits, NF-YA, NF-YB and NF-YC, and binds to CCAAT motifs in

the promoter regions of a variety of genes (18). NF-YA was reported to upregulate the expression of molecular chaperones. Our results demonstrate that NF-YA is also able to induce the expression of CHIP and TFEB, which suggests that NF-YA plays a pivotal role in the clearance of pathogenic proteins and the maintenance of proteostasis. The upregulation of diverse molecules involved in the proteolytic machinery must contribute to the marked beneficial effects of PF treatment in the AR-97Q mice. AR-97Q transgene expression decreased the expression of NF-YA, due to the decrease in mRNA levels (Fig. 6A and B) and sequestration of endogenous NF-YA in the inclusions (Supplemental Material, Fig. S6A and B). Consequently, the expression levels of molecular chaperones, CHIP and TFEB decreased in the spinal cord and muscle (Fig. 6C and D). The reduction of these molecules can impair the function of the proteolytic machinery and enhance polyQ toxicity. NF-YA also colocalized with mutant AR NIs that were present in the motor neurons and muscles of SBMA patients (Supplementary Material, Fig. S6A and B). NIs that were positive for NF-YA have been identified in models of SBMA (36), Huntington's disease (HD) (37) and spinocerebellar ataxia 17 (SCA17) (38), which suggests that NF-YA is a protein targeted for sequestration in polyQ diseases. Collectively, these data suggest that PF can increase the expression of NF-YA and restore the proteolytic machinery. It is likely that the proteolytic machinery is inhibited by misfolded proteins in the affected tissues of diverse polyQ diseases, such as SBMA, HD and SCA17 (36–38).

Mutant AR was preferentially degraded compared with wild-type AR in the presence of PF in both the cell culture and mouse models of SBMA. Mutant AR elimination was mediated by the upregulation of molecular chaperones and CHIP in which it was then prone to proteasomal degradation (39). Hsp70 and Hsp40 suppress aggregate formation and cellular toxicity in a wide range of polyQ disease models (30,40–43). CHIP interacts with Hsp90 or Hsp70 and ubiquitinates and degrades unfolded proteins trapped by molecular chaperones (44). A wide variety of proteins have been identified as CHIP substrates, including polyQ disease-causative proteins (45). Unfolded mutant proteins are more efficiently ubiquitinated by CHIP in the presence of molecular chaperones (12). Furthermore, mutant AR with a longer polyQ length is more efficiently ubiquitinated by CHIP (46). Based on these findings, the upregulation of CHIP expression by PF treatment may facilitate the preferential degradation of mutant AR in close cooperation with upregulated molecular chaperones.

Our experiments demonstrated that PF elevated the expression of TFEB and promoted the degradation of ARs via the activation of the autophagy system. AR has been demonstrated to be a direct target of autophagy (47,48). TFEB is a master regulator of lysosomal biogenesis and function (14) and upregulates lysosomal pathways and autophagy by modulating the expression of lysosomal enzymes involved in protein degradation (15). TFEB also regulates lysosomal proteostasis (49) and exocytosis (50). Importantly, TFEB regulates the clearance of disease-causing proteins, including huntingtin (14) and Aβ (51), and its overexpression reduces the expression level of polyQ-expanded huntingtin protein (52). However, chronically enhanced autophagy contributed to the detrimental consequences in the skeletal muscle of an SBMA mouse model (53). Although future studies should weigh the detrimental effects of chronically inducing autophagy to address proteinopathies against our observation of beneficially elevated autophagy in SBMA, sufficient inhibition of AR accumulation may overcome the deleterious effects of autophagy induction on muscle atrophy. Overall, based on our observations and taking the results from the previous studies into account, PF treatment promoted the degradation of both wild-type and mutant ARs by activating lysosomal biogenesis via the TFEB pathway and thereby restored the phenotypic defects in the SBMA mouse model. Collectively, PF treatment could provide a two-pronged cooperative therapeutic effect against SBMA pathogenesis by activating the molecular chaperone–UPS system and the autophagy system to degrade the mutant AR.

In conclusion, our present study demonstrated the safety and efficacy of PF in a mouse model of SBMA. PF potently induced the proteolytic machinery of UPS and autophagy, which lead to mutant AR degradation. In SBMA patients, the diffuse nuclear accumulation of mutant AR is frequent and extensive and occurs both in regions of the central nervous system and in muscles. The accumulation of pathogenic proteins causes many age-related neurodegenerative diseases. Inducers of the proteolytic machinery appear to be potent agents for disease-modifying therapies that inhibit the pathogenic process of neuron degeneration (54); thus, the pharmacological induction of the proteolytic machinery through PF treatment appears to be an applicable therapeutic strategy for multiple neurodegenerative disorders, including SBMA.

MATERIALS AND METHODS

Plasmid constructs and siRNA

pcDNA3.1/V5-His-NF-YA plasmid (37) was kindly provided by Dr Nobuyuki Nukina in the Department of Neuroscience for Neurodegenerative Disorders, Juntendo University Graduate School of Medicine. The plasmids pCR3.1-AR-24Q and pCR3.1-AR-97Q (32) were also used. The human TFEB cDNA was cloned into pcDNA 6.2/V5-GW/D-TOPO (Invitrogen) from the RNA of SH-SY5Y human neuroblastoma cells (ATCC No. CRL-2266). All of the constructs were verified by DNA sequencing. For the knock-down of NF-YA, 10 nM siRNA was used with the following sequence: 5′-CAGUAUCA CACCGCAUCCUUATT-3′ (sense) and 5′-UAAGGAUGCGG UGAUACUGTT-3′ (anti-sense). We used MISSION siRNA Universal Negative Control (Sigma) as the control siRNA.

Cell culture and DNA transfection

NSC34 cells were transfected using Lipofectamine 2000 (Invitrogen, Carlsbad, CA, USA) with plasmids encoding ARs containing normal (24 CAGs) or expanded (97 CAGs) polyQ repeats (32). Stable clones expressing these normal and mutant ARs were established by selection with the antibiotic G418 (0.4 mg/ml final concentration). The AR is not expressed in non-transfected NSC34 cells. All cell cultures were propagated in the absence of androgen. In western blots from these cultures, we detected a band of monomeric mutant AR in the separating gel but could hardly detect the high-molecular-weight mutant AR protein complex, which was retained in the stacking gel. Therefore, this cultured cell model is better suited for estimating the change in monomeric mutant AR expression.